11.1 Continuum- and Particle-Based Modeling of Human Red Blood Cells

Xuejin Li, Huijie Lu, and Zhangli Peng

Abstract Computational modeling and simulations can tackle a broad range of morphological, mechanical, and rheological problems relevant to blood and blood cells. Here, we review some continuum-based and particle-based computational approaches towards the modeling of healthy and diseased red blood cells (RBCs) with focus on the most recent contributions, including the three-level multiscale RBC model coupled with the boundary integral method of surrounding flows and two-component RBC models with explicit descriptions of lipid bilayer, cytoskeleton, and transmembrane proteins.

1 Introduction

Blood is a bodily fluid that delivers oxygen and nutrients to living cells and takes away metabolic waste products from those same cells. It is composed of blood cells suspended in blood plasma, which makes up about 55% of the volume of whole blood. Blood plasma is the liquid component of blood, which contains mostly water and other substances like dissolved proteins, glucose and clotting factors. Blood cells are mainly red blood cells (also called erythrocytes or RBCs), white blood cells

Xuejin Li
Division of Applied Mathematics, Brown University, Providence, RI 02912, USA; Institute of Fluid Engineering, Zhejiang University, Hangzhou, Zhejiang 310027, P. R. China. e-mail: Xuejin_Li@brown.edu

Huijie Lu
Department of Aerospace and Mechanical Engineering, University of Notre Dame, Notre Dame, IN 46556, USA. e-mail: hlu3@nd.edu

Zhangli Peng
Department of Aerospace and Mechanical Engineering, University of Notre Dame, Notre Dame, IN 46556, USA. e-mail: zpeng3@nd.edu

(also called leukocytes or WBCs), and plasma (also called thrombocytes). Taking together, these three kinds of blood cells add up to a total 45% of the volume of whole blood. In particular, RBCs are the most common type of blood cells, with each cubic millimeter (1 mm^3) of blood containing about 4-6 million RBCs.

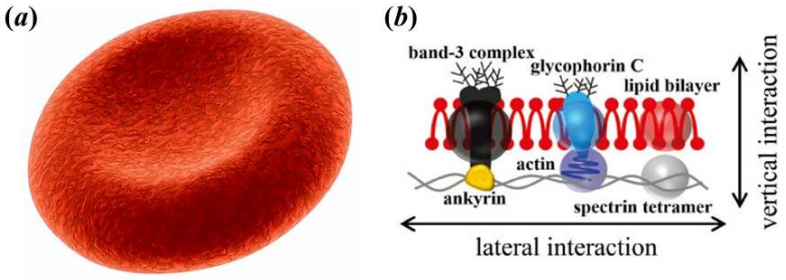

Fig. 1 Schematic representation of the morphology of (*a*) a normal RBC and (*b*) its two-component membrane structure (Li et al 2017a).

A normal RBC is a nucleus-free cell; it is essentially a cell membrane encapsulating a hemoglobin solution. Upon maturation, it adopts a unique biconcave shape of approximately 8.0 μm in diameter and 2.0 μm in thickness (Fig. 1*a*). The RBC membrane consists three basic components: a lipid bilayer, a cytoskeletal network and transmembrane proteins such as glycophorins AD, band 3, and some substoichiometric glycoproteins (e.g., CD44, CD47) (Fig. 1*b*). The deformability of an RBC is determined by the elasticity, geometry and viscosity of the RBC membrane. A normal RBC is highly deformable allowing it to squeeze through capillaries as small as 3 microns in diameter without any damage. Several pathological conditions, including malaria, sickle cell disease, hereditary spherocytosis and elliptocytosis, can alter the shape and deformability of circulating RBCs, leading to possible vascular obstruction. Over the past few decades, computational models, such as continuum-based and particle-based RBC models, have been proven to be an important tool in accurately resolving a broad range of biological problems associated with RBCs (Abkarian and Viallat 2008, Vlahovska et al 2011, Li et al 2013, 2017b). Actually, there is a great variety of modeling approaches since no universal solution for all blood flow related problems. In this chapter, we overview the computational approaches towards the modeling of RBCs focusing on the most recent contributions.

For the most problems, the surrounding blood plasma plays a significant role in the RBC dynamics. The accurate modeling of the fluid-structure interaction between the RBCs and the surrounding flow is crucial to predict the physics. There are three major groups of numerical methods in the existing literature to study motion and deformation of RBCs in flow (Pozrikidis 2010, Barthès-Biesel 2016, Freund 2014). In the first group of methods, boundary integral equations are used to represent the Stokes flow and coupled to the membrane (Walter et al 2010, Pozrikidis

1992), which is usually modeled as meshes or spectral elements (Zhao et al 2010) either by enforcing the membrane equilibrium equation directly (Pozrikidis 1992) or by the finite element method based on the virtual work principle (Walter et al 2010, Peng et al 2011). This type of methods has been known to be very precise in various studies of simple shear flow and plane hyperbolic flow (Barthès-Biesel 2016, Freund 2014). In the second group of the immerse-boundary type methods, the fluid domain is solved using either the finite difference method (Yazdani et al 2011) or the lattice Boltzmann method (LBM) (Sui et al 2008), and the capsule membrane is solved using continuum methods such as finite element method (FEM). The force from capsule membrane nodes is distributed to the fluid domain as Dirac delta functions, which are approximated by smooth functions sharply varying over a few fixed grid meshes. The precision of these methods may be reduced as the methods do not treat the membrane as physical boundaries but as approximated Dirac functions. In the third group, particle methods such as dissipative particle dynamics (DPD) Pivkin and Karniadakis (2008), Peng et al (2013), multi-particle collision dynamics (MPCD) (Noguchi and Gompper 2005, McWhirter et al 2009), and smoothed particle hydrodynamic (SPH) method (Hosseini and Feng 2012) are used, and the capsule and RBC membranes are modeled as triangular networks of particles with bond, angle, and dihedral interactions (Discher et al 1998). In addition to these three groups, phase-field methods (Du et al 2004) and arbitrary Lagrangian Eulerian (ALE) method using FEM (Barber et al 2011, Ni et al 2015) are used as well to study capsules and vesicles.

2 Continuum-based models

Continuum-based models provided useful insights in many aspects of RBC mechanics by adopting the robust and accurate numerical methods developed in the well established continuum mechanics community Barthès-Biesel (2016). The cell membrane is typically 7.5-10 *nm* in thickness; hence it is usually treated as a two-dimensional viscoelastic material embedded in a three-dimensional space. Traditionally, continuum-based RBC models treat RBC membrane and intracellular hemoglobin solution as homogeneous materials, using boundary integral method (BIM) (Ramanujan and Pozrikidis 1998, Lac et al 2004, Zhao et al 2010, Veerapaneni et al 2011), immersed boundary method (IBM) (Peskin 2002, Doddi and Bagchi 2009, Yazdani and Bagchi 2011, Fai et al 2013), and fictitious domain method (FDM) (Shi et al 2014, Hao et al 2015). These continuum-based models describe the modeling system using locally-averaged variables, such as density, stress, and velocity, with ordinary and partial differential equations governing flow dynamics and fluid mechanics. Blood flow in microcirculation normally falls in the Stokes regime where inertial effects are negligible, hence making BIM a popular technique for addressing multiphase flow problems. The BIM method exploits the fact that the equations of fluid motion are linear and can be recast into an integral equation for the evolution of the interface (Ramanujan and Pozrikidis 1998, Lac et al

2004, Zhao et al 2010, Veerapaneni et al 2011). Among other continuum solvers, the IBM has become very effective in addressing fluid-structure problems (Peskin 2002, Fai et al 2013). There are several numerical extensions of IBM depending on the choice of the structural and fluid formulations. For example, the front-tracking method (Doddi and Bagchi 2009, Yazdani and Bagchi 2011) used a first-order finite element triangulation of cell membrane, while the full Navier-Stokes equation has been solved using projection splitting scheme. More recently, FDM for solving coupled fluid-structure systems by introducing a Lagrange multiplier over the solid domain has been used (Shi et al 2014, Hao et al 2015). This multiplier acts as a penalty term that imposes the kinematic constraint in the solid domain. Another computational challenge is to include the membrane thermal undulations; progress in this direction has been made by introducing a stochastic formulation for IBM (Atzberger et al 2007).

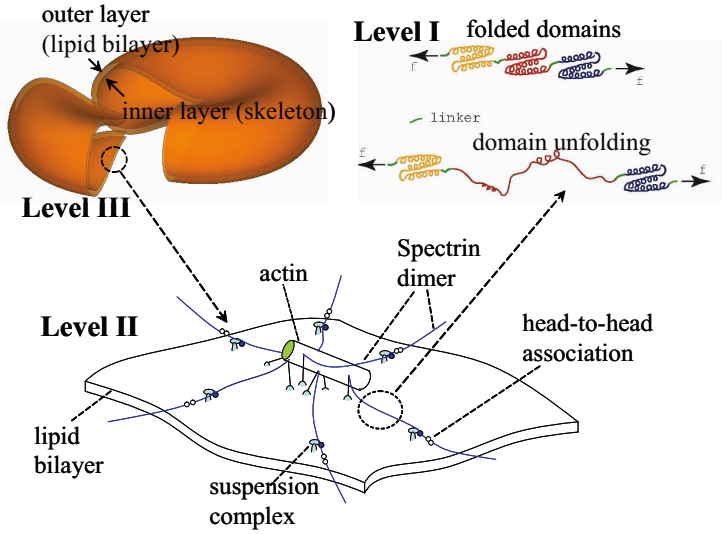

Fig. 2 Two-component RBC model using three-level hierarchical multiscale continuum method (Peng et al 2010).

These continuum-based RBC models allow the study of blood flow dynamics on macroscopic length and time scales. However, the RBC membrane is considered as a uniform continuum media in these continuum models, and the detailed molecular structure was not considered. Recently, multiscale RBC models that include sufficient molecular details have been developed. For example, Peng et al. have developed a three-level multiscale model of RBCs and coupled it with a boundary element model to study the dynamic response of RBCs in tube and shear flows (Peng et al 2010). For the RBC membrane, we built a three-level multiscale model to simulate its viscoelastic behaviors at different length scales, including single protein

scale, protein complex scale and cell scale. For the fluids surrounding the RBC, we used a boundary element approach to study the fluid dynamics based on the Stokes equation of viscous flow (Peng et al 2011).

The dynamics of RBCs involves physics at different length scales. For example, in the whole cell level, RBCs may undergo tank-treading motions in shear flow in the micro meter scale (Fischer et al 1978, Tran-Son-Tay et al 1984). In the protein complex scale, junctional complexes of RBCs may experience fluctuations due to mode switching (Lee and Discher 2001, Zhu et al 2007). In the protein level, tension may induce spectrin unfolding in the nanoscale (Rief et al 1999, Zhu et al 2007). We developed a multiscale framework to investigate the physics in different length scales, including three models at three different length scales, and coupled them together using a hierarchical multiscale approach, as shown in Fig. 2.

At Level I, Zhu and Asaro developed a model of spectrin using Monte-Carlo simulation (Zhu and Asaro 2008). Spectrin is the major RBC cytoskeleton protein that forms a triangular network. Rief et al. applied AFM to stretch a single spectrin and found that it can be modeled accurately using a nonlinear constitutive model called worm-like chain (WLC) (Rief et al 1999, Discher et al 1998, Li et al 2005). Besides that, it was found that if the spectrin is stretched beyond its contour length, multiple protein domains may unfold to increase the contour length. In order to capture the full mechanical behavior of the spectrin, Zhu and Asaro took into account its domain unfolding feature by employing a Monte-Carlo method, as the probability of the unfolding is a function of the loading (Zhu and Asaro 2008). By simulating the unfolding of the spectrin, Zhu and Asaro got consistent force-displacement curves as in the AFM experiment (Rief et al 1999). In addition, the effect of stretching rate is also quantified. After these force-displacement curves are obtained, the information is passed as a database to the next level model (Level II).

At Level II, Zhu et al. developed a 3D junctional complex model with molecular details using Brownian dynamics (BD), which is a basic protein complex unit in the RBC cytoskeleton (Zhu et al 2007). In the junctional complex, an actin protofilament is associated with six or five spectrins. Zhu et al. built an exact geometry model based on the state-of-the-art understanding of the molecular structure of a junctional complex, including the binding sites between spectrins and actins (Sung and Vera 2003). They simulated thermal fluctuations of the RBC membrane using this model (Zhu et al 2007), and predicted the area and shear moduli of the cytoskeleton, as functions of membrane deformation (Zhu et al 2007, Peng et al 2010), which can be passed to the next cell level model (Level III).

At Level III, Peng et al. developed a whole cell model of RBCs using finite element method (FEM) and considered the normal and tangential interactions between the lipid bilayer and the cytoskeleton (Peng et al 2010, 2011). The cytoskeleton may slide against the lipid bilayer (Fischer 1992, Dodson III and Dimitrakopoulos 2010), since the cytoskeleton is connected to the lipid bilayer through transmembrane proteins such as band 3 and glycophorin C, which can move freely within the lipid bilayer. In order to describe the bilayer–cytoskeletal interaction accurately, we modeled the RBC membrane as two distinct layers. We employed an inner layer to present the cytoskeleton with finite area and shear stiffnesses, and negligible bend-

ing stiffness, and an outer layer to represent the lipid bilayer with zero shear stiffness, huge area stiffness, and significant bending stiffness. Vertical elastic interaction and tangential viscous friction between the lipid bilayer and the cytoskeleton are simulated using a contact algorithm based on the penalty method (Malone and Johnson 1994). The bilayer–cytoskeletal friction coefficient is estimated based on the Stokes-Einstein relation and experimentally measured diffusivities of band 3 and glycophorin C in the lipid bilayer (Kapitza et al 1984, Kodippili et al 2009, Tomishige 1998). Reduced integration shell elements based on Mindlin theory were used to simulate both the outer and the inner layers (Peng et al 2010).

Besides the elasticity, we also considered the viscosities of the lipid bilayer and the cytoskeleton, which play significant roles in dynamics processes such as tank-treading. For example, it has been demonstrated that without considering the membrane viscosity, the predicted tank-treading frequency cannot match the experimental measurement (Fedosov et al 2011a, Peng et al 2011). Different from the existing study (Fedosov et al 2011a), we consider the viscosities of the lipid bilayer and the cytoskeleton separately using a generalized Voigt-Kelvin stress-strain relation (Evans and Skalak 1980). Furthermore, we modeled the sliding between the bilayer and the skeleton as a viscous friction force. The viscous fluids surrounding the cell are incorporated in the following boundary element model of Stokes flow.

We applied a boundary element method to simulate the Stokes flows inside and outside of the RBC and coupled it with FEM to study the fluid-structure interaction. We used a staggered algorithm with explicit time integration (Peng et al 2011). For the interface dynamics in the Stokes flow with zero Reynolds number, we applied the boundary integral equation (Pozrikidis 1992) so that the velocity $\mathbf{v}^f$ is given as

$$\begin{aligned}\mathbf{v}^f(\mathbf{x}_0) &= \frac{2}{1+\Lambda}\bar{\mathbf{v}}^f(\mathbf{x}_0)\\ &- \frac{1}{4\pi\eta_1(\Lambda+1)}\int_{\Gamma^{fb}}\mathbf{G}(\mathbf{x},\mathbf{x}_0)\cdot\Delta\mathbf{t}^f(\mathbf{x})d\Gamma(\mathbf{x})\\ &+ \frac{1-\Lambda}{4\pi(1+\Lambda)}\iint\!\!\!\!\!\!-_{\Gamma^{fb}}\mathbf{v}^f(\mathbf{x})\cdot\mathbf{T}(\mathbf{x},\mathbf{x}_0)\cdot\mathbf{n}(\mathbf{x})d\Gamma(\mathbf{x}),\end{aligned} \tag{1}$$

where Γ^{fb} is the membrane surface and $\bar{\mathbf{v}}^f$ is the prescribed undisturbed velocity field of the shear flow. The vector $\Delta\mathbf{t}^f = \mathbf{t}^{f,1} - \mathbf{t}^{f,2}$ is the discontinuity in the interfacial surface traction, where $\mathbf{t}^{f,1}$ is the traction in the outside surface $\Gamma^{fb,1}$ of the interface, and $\mathbf{t}^{f,2}$ is the traction in the inside surface $\Gamma^{fb,2}$ of the interface. The surface traction is related to the nodal force through the principle of virtual work (Walter et al 2010). $\iint\!\!\!\!\!\!-$ denotes the principal value integration.

$\mathbf{G}$ is the Green's function for velocity. Its components are

$$G_{ij}(\mathbf{x},\mathbf{x}_0) = \frac{\delta_{ij}}{|\mathbf{x}-\mathbf{x}_0|} + \frac{(x_i - x_{0_i})(x_j - x_{0_j})}{|\mathbf{x}-\mathbf{x}_0|^3}, \tag{2}$$

where δ_{ij} is Kronecker's delta. $\mathbf{T}$ is the Green's function for stress. It can be written as

$$T_{ijk}(\mathbf{x},\mathbf{x}_0) = -6\frac{(x_i - x_{0_i})(x_j - x_{0_j})(x_k - x_{0_k})}{|\mathbf{x}-\mathbf{x}_0|^5}. \quad (3)$$

Extensive validations have been conducted in each level to verify the models, such as optical tweezers stretching (Peng et al 2010), micropipette aspiration (Peng et al 2010), tank-treading and tumbling of RBCs in shear flow(Peng et al 2011). More importantly, the effect of stress-free cytoskeleton state on the tank-treading behavior has been compared with the available experiments in details (Dupire et al 2012, Peng et al 2014, 2015). Besides validations, we predicted correlation between the occurrence of spectrin unfolding and increase in the mechanical load upon individual skeleton–bilayer pinning points and related it to the vesiculation process (Knowles et al 1997). The simulation results also show that during tank-treading the protein density variation is insignificant for healthy RBCs, but significant for cells with a smaller bilayer–cytoskeletal friction coefficient, which may be the case in hereditary spherocytosis (Walensky et al 2003). We also predicted two different modes of motions for RBCs in shear flow (Peng and Zhu 2013) and studied the effect of stress-free state on the tank-treading motion (Peng et al 2014, 2015, Dupire et al 2012). We showed that the cell maintains its biconcave shape during tank-treading motions under low shear rate flows, by employing a spheroidal stress-free state in the cytoskeleton (Peng et al 2014). Furthermore, we numerically confirmed the hypothesis that, as the stress-free state approaches a sphere, the threshold shear rates corresponding to the establishment of tank treading decrease. By comparing with the experimental measurements (Dupire et al 2012), our study suggests that the stress-free state of RBCs is a spheroid that is close to a sphere, rather than the biconcave shape applied in existing models (Peng et al 2014). In addition, we also quantified the stability phase diagram of different motion modes in high shear rate flows and explored the effect of stress-free state on the phase diagram (Peng et al 2015).

3 Particle-based models

Particle-based models treat both the fluid and the cell membrane as particulate materials, and they can model critical biophysical processes involving the RBCs at cellular and sub-cellular scales, such as membrane fluctuations and the defective membrane structure. Several particle-based RBC models, including molecular-detailed composite RBC models (Li and Lykotrafitis 2012, 2014, Tang et al 2017) and coarse-grained RBC models (Discher et al 1998, Li et al 2005, Noguchi and Gompper 2005, Pivkin and Karniadakis 2008, Pan et al 2010, Fedosov et al 2010, Peng et al 2013), have been developed and employed to quantify the structural, mechanical, and rheological properties of RBCs in health and disease.

Generally, the molecular-detailed composite RBC models describe explicitly lipid bilayer, cytoskeleton, and transmembrane proteins using coarse-grained molecular dynamics (CGMD) (Li and Lykotrafitis 2012, 2014). They are able to capture the membrane-related structural problems in RBCs. Specifically, the spectrin

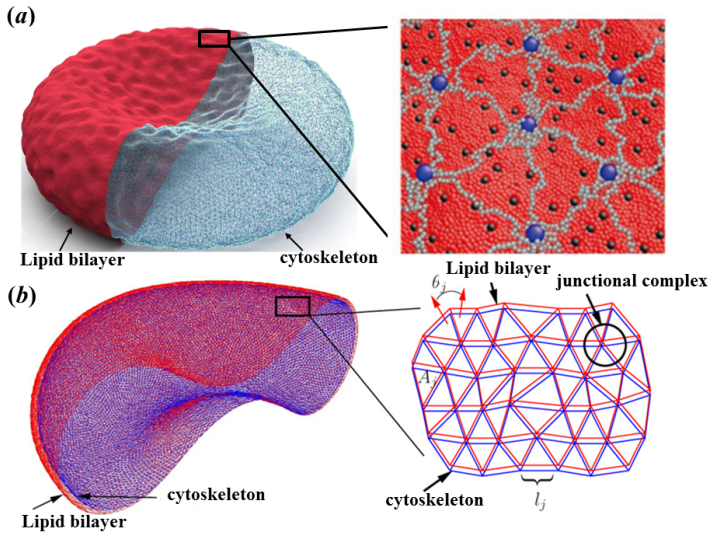

Fig. 3 Two-component RBC model at protein resolution(Tang et al 2017, Li and Lykotrafitis 2014) and coarse-grained level (Peng et al 2013).

tetramer in the the composite membrane model is represented by a chain of 39 beads (grey particles in Fig. 3a) connected by spring bonds (Li et al 2007). The corresponding potential has the form,

$$V_{cy}^{s-s} = \frac{1}{2}k_0(r - r_{eq}^{s-s})^2 \tag{4}$$

where k_0 and r_{eq}^{s-s} are the spring constant and equilibrium distance between two spectrin particles, respectively. Spectrin particles that are not connected by the spring potential interact with each other via the repulsive term of Lennard-Jones potential, given by

$$V_{rep}(r_{ij}) = \begin{cases} 4\varepsilon\left[\left(\frac{\sigma_{ij}}{r_{ij}}\right)^{12} - \left(\frac{\sigma_{ij}}{r_{ij}}\right)^{6}\right] + \varepsilon & r_{ij} < r_{eq}^{s-s} \\ 0 & r_{ij} \geq r_{eq}^{s-s} \end{cases} \tag{5}$$

where ε is the energy unit and σ_{ij} is the length unit, and r_{ij} is the distance between spectrin particles. To couple the lipid bilayer and spectrin network, actin junctional complexes are connected to the glycophorin C and the middle beads of the spectrin network are bonded to the band-3 complexes which are specifically rendered in yellow particles. These bonds are modeled as harmonic springs, given by

$$V_{cy}^{a-s} = \frac{1}{2}k_0(r - r_{eq}^{a-s})^2 \tag{6}$$

where r_{eq}^{a-s} = 10 nm is the equilibrium distance between an actin and a spectrin particle.

These molecular-detailed composite membrane models have been successfully to study some issues associated with RBC membrane defects, such as the multiple stiffening effects of nanoknobs on malaria-infected RBCs (Zhang et al 2015, Chang et al 2016), the vesiculation of mature RBCs in hereditary elliptocytosis and spherocytosis (Li and Lykotrafitis 2015), and the diffusion of transmembrane proteins in normal and defective RBC membrane (Li et al 2016). However, modeling only a portion of the RBC membrane does not efficiently depict the whole-cell characteristics strongly related to RBC mechanics and rheology.

More recent efforts have focused on this approach, leading to a two-component whole-cell model (OpenRBC) at protein resolution with explicit descriptions of lipid bilayer, cytoskeleton, and transmembrane proteins (Fig. 3a) (Tang et al 2017). In the OpenRBC, the modeled RBC is generated from a triangular mesh of cytoskeleton that resembles the biconcave disc shape of a normal RBC, where the lipid molecules and mobile band-3 particles are randomly placed on triangular faces. The modeled RBC system is also optimized by a velocity quenching algorithm to avoid the overlap of particles. It can simulate an entire RBC with a resolution down to single protein level, which offers unique tools for the qualitative and quantitative predictions of dynamic and mechanical properties of healthy and pathological RBCs beyond available experimental measurements, such as the vesiculation of RBCs in hereditary spherocytosis and elliptocytosis (Tang et al 2017), and rupture of RBCs in splenic passage (Li et al 2018). However, at present, they are computationally very expensive for large-scale applications such as modeling whole blood involving a large number of RBCs. On the other hand, coarse-grained whole-cell model provides the opportunity to significantly reduce the computational complexity. For example, a three-dimensional multiscale RBC (MS-RBC) model has been developed and successfully applied to RBC simulations at different length scales (Pivkin and Karniadakis 2008, Fedosov et al 2010).

In the MS-RBC model, the cell membrane is modeled by a 2D triangulated network with N_v vertices connected by springs, where each vertex is represented by a DPD particle. The RBC membrane model takes into account the elastic energy, bending energy, and constraints of fixed surface area and enclosed volume, which is defined as

$$V = V_s + V_b + V_a + V_v \tag{7}$$

where V_s is the elastic energy that mimics the elastic spectrin network, given by

$$V_s = \sum_{i \in \text{springs}} \left[\frac{k_B T l_m}{4p} \frac{3x_i^2 - 2x_i^3}{1 - x_i} \right] + \sum_{\alpha \in \text{triangles}} \frac{1}{A_\alpha} \left[\frac{3\sqrt{3} k_B T l_m^3 x_0^4}{64p} \frac{4x_0^2 - 9x_0 + 6}{(1 - x_0^2)} \right], \tag{8}$$

where $k_B T$ is the energy unit, A_α is the area of triangle α formed by three vertices. Also, $x_i = l_i/l_m$, $x_0 = l_0/l_m$, where l_i is the length of spring i, l_0 and l_m are the

equilibrium spring length and maximum spring extension, and p is the persistence length.

The cell membrane viscoelasticity is imposed by introducing a viscous force on each spring, which has the form,

$$\mathbf{F}_{ij}^{D} = -\gamma^{T}\mathbf{v}_{ij} - \gamma^{C}(\mathbf{v}_{ij}\cdot\mathbf{e}_{ij})\mathbf{e}_{ij}, \tag{9}$$

$$\mathbf{F}_{ij}^{R}dt = \sqrt{2k_{\mathrm{B}}T}\left(\sqrt{2\gamma^{T}}d\overline{\mathbf{W}_{ij}^{S}} + \sqrt{3\gamma^{C}-\gamma^{T}}\frac{tr[d\mathbf{W}_{ij}]}{3}\mathbf{1}\right)\cdot\mathbf{e}_{ij}, \tag{10}$$

where γ^{T} and γ^{C} are dissipative parameters; $\mathbf{v}_{ij}$ is the relative velocity of spring ends, and $d\overline{\mathbf{W}_{ij}^{S}} = d\mathbf{W}_{ij}^{S} - tr[d\mathbf{W}_{ij}^{S}]\mathbf{1}/3$ is the traceless symmetric part of a random matrix representing the Wiener increment.

The bending resistance of the RBC membrane is modeled by

$$V_b = \sum_{\alpha,\beta\ \text{pair}} k_b\left[1-\cos(\theta_{\alpha\beta}-\theta_0)\right], \tag{11}$$

where k_b is the bending modulus constant, $\theta_{\alpha\beta}$ is the instantaneous angle between two adjacent triangles having common edge, and θ_0 is the spontaneous angle. In addition, the RBC model includes the area and volume conservation constraints, which mimic the area-incompressibility of the lipid bilayer and the incompressibility of the interior fluid, respectively. The corresponding energy terms are given by

$$V_a = \frac{k_a k_B T(A-A_0)^2}{2l_0^2 A_0}, \quad V_v = \frac{k_v k_B T(V-V_0)^2}{2l_0^3 V_0} \tag{12}$$

where k_a and k_v are the area and volume constraint coefficients. Here A_0 and V_0 are the equilibrium area and volume of a cell, respectively.

The MS-RBC model is multiscale, as the RBC can be represented on the spectrin level, where each spring in the network corresponds to a single spectrin tetramer with the equilibrium distance between two neighboring actin connections of ~ 75 *nm*. On the other hand, for more efficient computations, the RBC network can also be highly coarse-grained with the equilibrium spring lengths of up to 500$\sim$600 *nm*. In addition, being constructed from a coarse-grained molecular dynamics (CGMD) approach, the MS-RBC model can naturally include membrane thermal fluctuations (Fedosov et al 2011b, Chang et al 2017). Such formulations are compatible with coarse-grained mechanical descriptions of the RBC membrane with the advantage of including the viscosity of the RBC membrane without additional cost. Thus, the particle-based whole-cell models can resolve subcellular and cellular scales.

A two-component particle-based whole-cell model, which separately accounts for the lipid bilayer and cytoskeleton but implicitly includes the transmembrane proteins, has been developed and implemented using DPD (Fig. 3b) (Peng et al 2013).

In this two-component whole-cell model, the cell membrane is modeled by two distinct components, i.e., the lipid bilayer and the spectrin network. Specifically, through the DPD approach, each component is constructed by a two-dimensional triangulated network, which is analogous to the one-component whole-cell model; however, the lipid bilayer of the two-component whole-cell model has no shear stiffness at healthy state but only bending stiffness and a very large local area stiffness, whereas the cytoskeleton has no bending stiffness but possesses a finite shear stiffness. In addition, this unique two-component whole-cell model takes into account the bilayer-cytoskeleton interaction potential, which is expressed as a summation of harmonic potentials given by

$$V_{int} = \sum_{j,j' \in 1 \ldots N_{bs}} \frac{k_{bs}(d_{jj'} - d_{jj',0})^2}{2}, \tag{13}$$

where k_{bs} and N_{bs} are the spring constant and the number of bond connections between the lipid bilayer and the cytoskeleton, respectively. $d_{jj'}$ is the distance between the vertex j of the cytoskeleton and the corresponding projection point j' on the lipid bilayer, with the corresponding unit vector $\mathbf{n}_{jj'}$; $d_{jj',0}$ is the initial distance between the vertex j and the point j', which is set to zero in the current simulations. Physical view of the local bilayer-cytoskeleton interactions include the major connections via band-3 complex and ankyrin, as well as the secondary connections via glycophorin C and actin junctions, here we consider them together as an effective bilayer-cytoskeleton interaction and model it as a normal elastic force, $\mathbf{f}^E_{jj'}$, and a tangential friction force, $\mathbf{f}^F_{jj'}$. The corresponding elastic force on the vertex j of the cytoskeleton is given by

$$\mathbf{f}^E_{jj'} = \begin{cases} k_{bs}(d_{jj'} - d_{jj',0})\mathbf{n}_{jj'} & d_{jj'} < d_c \\ 0 & d_{jj'} \geq d_c \end{cases} \tag{14}$$

where $d_c \approx 0.2\ \mu m$ is the cutoff distance. The tangential friction force between the two components is represented by

$$\mathbf{f}^F_{jj'} = -f_{bs}[\mathbf{v}_{jj'} - (\mathbf{v}_{jj'} \cdot \mathbf{n}_{jj'})\mathbf{n}_{jj'}], \tag{15}$$

where f_{bs} is the tangential friction coefficient and $\mathbf{v}_{jj'}$ is the difference between the two velocities.

The two-component whole-RBC model is capable of simulating the interactions between the lipid bilayer and the cytoskeletal network of human RBCs (Peng et al 2013, Li et al 2014, Chang et al 2016). Furthermore, it is computationally more efficient than the two-component OpenRBC model for blood flow modeling. Herein, the two-component whole-cell RBC model has been used in simulations of blood flow and quantified the existence of bilayer-cytoskeletal slip for RBC membrane in pathological state (Peng et al 2013, Li et al 2014).

4 Summary

To summarize the continuum-based and particle-based models of RBCs, we list the main features and applications of some existing mesoscale RBC models in Table 1. The main differences are the molecular details considered and the length scales these model can reach. The two-component CG model focused on the detailed bilayer–cytoskeletal interaction and transmembrane protein diffusion, but it is too expensive to employ it to study a whole cell with current methodology. The two-component DPD model studied the whole cell behavior and explored the bilayer–cytoskeletal interaction in a simplified way. The three-level multiscale approach is developed to bridge three models in different length scales, but due to the information passing, some information is lost, such as the thermal fluctuations in the whole cell level.

Table 1 Comparison of different RBC models.

RBC Models	Main Characteristics	Examples of Application
Two-component CGMD composite model (Li and Lykotrafitis 2012, 2014, Zhang et al 2015)	• One-particle-thick bilayer model • Small piece of membrane	➢ Transmembrane protein diffusion ➢ RBC membrane defects ➢ RBC membrane vesiculation
Three-level multiscale model (Peng et al 2010, 2011)	• FEM, LD and MC • Spanning from protein to cell	➢ Micropipette vesiculation ➢ Dynamics of junctional complexes ➢ Spectrin unfolding
OpenRBC model (Tang et al 2017)	• One-particle-thick bilayer model • Bilayer-cytoskeletal interaction • Whole-cell level	➢ RBC vesiculation ➢ RBC lysis
One-component DPD model (Pivkin and Karniadakis 2008, Fedosov et al 2010)	• Coupled with fluids • Systematic coarse-graining • Whole-cell level	➢ Membrane thermal fluctuations, ➢ Tank-treading motion ➢ Microfluidics
Two-component DPD model (Peng et al 2013, Li et al 2014)	• Bilayer-cytoskeletal interaction • Whole-cell level	➢ Bilayer--cytoskeletal slip ➢ Bilayer tethering ➢ Membrane thermal fluctuations
Two-component MPCD model (Noguchi and Gompper 2005, McWhirter et al 2009)	• Coarse-graining model • Whole-cell level	➢ Tube flow ➢ Tank-treading motion
LBM model (Zhang et al 2008, Reasor et al 2012)	• Fluid-structure interaction • Whole-cell level	➢ Blood rheology ➢ Cell margination
Continuum model (Ramanujan and Pozrikidis 1998, Dao et al 2003, Yazdani and Bagchi 2011Freund 2013)	• Uniform property • No molecular details	➢ Large-scale blood flow modeling ➢ Tank-treading ➢ Optical tweezers stretching

There are still plenty of room to improve these models. For example, only one-way coupling has been done for the three-level multiscale RBC model, and two-way coupling can be added to study how the deformation in the macroscale can influence the dynamics of the proteins in the microscale. In addition, future effort will be put on how to improve the efficiency of the two-component CGMD RBC model in order to apply it in the whole cell scale and couple it with fluid motion. Such simulations could shed light on the coupling of biology, chemistry, and mechanics (the

"triple-point"). To make model predictions more reliable, it would require further mesoscopic validation and reliability testing of these models against experimental and clinical studies. Moreover, smoothed dissipative particle dynamics (SDPD) and smoothed particles hydrodynamics (SPH) have been also applied to study RBCs models (Hosseini and Feng 2012, Fedosov et al 2014, Muller et al 2015). Compared to conventional DPD, SDPD adopt advantages from smoothed particles hydrodynamics (SPH) (Van Liedekerke et al 2013), such as thermal consistency and specification of viscosity.

Since the RBC is a model system for cell mechanics and biological membranes, RBC models can be applied in other systems as well. For example, recently we extended the two-component RBC DPD model to study the blood vessel walls by considering the isotropic matrix and the anisotropic collagen fibers separately (Witthoft et al 2016). Furthermore, we can also apply RBC models to study the lipid bilayer and the actin cortex network or the intermediate filament network in general eukaryotic cells, because some of them share similar structures as the spectrin network of RBCs, such as the auditory outer hair cells and the nucleus lamina (Alberts et al 2002, Boal 2012).

Acknowledgements XL is supported in part by the National Institutes of Health (NIH) under grants U01HL114476 and U01HL116323. ZP and HL are supported in part by the National Science Foundation (NSF) under the grant CBET1706436.

References

Abkarian M, Viallat A (2008) Vesicles and red blood cells in shear flow. Soft Matter 4:653

Alberts B, Johnson A, Lewis J, Raff M, Roberts K, Walter P (2002) Molecular biology of the cell. Garland Science, New York, NY

Atzberger PJ, Kramer PR, Peskin CS (2007) A stochastic immersed boundary method for fluid-structure dynamics at microscopic length scales. J Comput Phys 224:1255–1292

Barber JO, Restrepo JM, Secomb TW (2011) Simulated red blood cell motion in microvessel bifurcations: Effects of cell–cell interactions on cell partitioning. Cardiovasc Eng Technol 2(4):349–360

Barthès-Biesel D (2016) Motion and deformation of elastic capsules and vesicles in flow. Annu Rev Fluid Mech 48:25–52

Boal D (2012) Mechanics of the Cell, 2nd edn. Cambridge University Press, Cambridge, UK

Chang HY, Li X, Li H, Karniadakis GE (2016) Md/dpd multiscale framework for predicting morphology and stresses of red blood cells in health and disease. PLoS Comput Biol 12(10):e1005,173

Chang HY, Li X, Karniadakis GE (2017) Modeling of biomechanics and biorheology of red blood cells in type 2 diabetes mellitus. Biophys J 113(2):481–490

Discher DE, Boal DH, Boey SK (1998) Simulations of the erythrocyte cytoskeleton at large deformation. ii. micropipette aspiration. Biophys J 75:1584–1597

Doddi SK, Bagchi P (2009) Three-dimensional computational modeling of multiple deformable cells flowing in microvessels. Phys Rev E 79(4):046,318

Dodson III WR, Dimitrakopoulos P (2010) Tank-treading of erythrocytes in strong shear flows via a nonstiff cytoskeleton-based continuum computational modeling. Biophys J 99:2906–2916

Du Q, Liu C, Wang X (2004) A phase field approach in the numerical study of the elastic bending energy for vesicle membranes. J Comput Phys 198(2):450–468

Dupire J, Socol M, Viallat A (2012) Full dynamics of a red blood cell in shear flow. Proc Natl Acad Sci USA 109:20,808–20,813

Evans E, Skalak P (1980) Mechanics and thermodynamics of biomembranes. CRC Press, Boca Raton, FL

Fai TG, Griffith BE, Mori Y, Peskin CS (2013) Immersed boundary method for variable viscosity and variable density problems using fast constant-coefficient linear solvers I: Numerical method and results. SIAM J Sci Comput 35(5):B1132–B1161

Fedosov D, Peltomaki M, Gompper G (2014) Deformation and dynamics of red blood cells in flow through cylindrical microchannels. Soft Matter 10:4258–4267

Fedosov DA, Caswell B, Karniadakis GE (2010) A multiscale red blood cell model with accurate mechanics, rheology, and dynamics. Biophys J 98:2215–2225

Fedosov DA, Caswell B, Karniadakis GE (2011a) Wall shear stress-based model for adhesive dynamics of red blood cells in malaria. Biophys J 100:2084–2093

Fedosov DA, Lei H, Caswell B, Suresh S, Karniadakis GE (2011b) Multiscale modeling of red blood cell mechanics and blood flow in malaria. PLoS Comput Biol 7:e1002,270

Fischer TM (1992) Is the surface area of the red cell membrane skeleton locally conserved? Biophys J 61:298–305

Fischer TM, Stohr-Liesen M, Schmid-Schonbein H (1978) The red cell as a fluid droplet: tank tread-like motion of the human erythrocyte membrane in shear flow. Science 202:894–896

Freund JB (2014) Numerical simulation of flowing blood cells. Annu Rev Fluid Mech 46(1):67–95

Hao W, Xu Z, Liu C, Lin G (2015) A fictitious domain method with a hybrid cell model for simulating motion of cells in fluid flow. J Comput Phys 280:345–362

Hosseini S, Feng J (2012) How malaria parasites reduce the deformability of infected red blood cells. Biophy J 103:1–10

Kapitza H, Rupped D, Galla H, Sackmann E (1984) Lateral diffusion of lipids and glycophorin in solid phosphatidylcholine bilayers. the role of structural defects. Biophys J 45:577

Knowles DW, Tilley L, Mohandas N, Chasis JA (1997) Erythrocyte membrane vesiculation: model for the molecular mechanism of protein sorting. Proc Natl Acad Sci USA 94:12,969–12,974

Kodippili G, Spector J, Sullivan C, Kuypers F, Labotka R, Gallagher P, Ritchie K, Low P (2009) Imaging of the diffusion of single band 3 molecules on normal and mutant erythrocytes. Blood 113:6237

Lac E, Barthes-Biesel D, Pelekasis N, Tsamopoulos J (2004) Spherical capsules in three-dimensional unbounded stokes flows: effect of the membrane constitutive law and onset of buckling. J Fluid Mech 516:303–334

Lee JC, Discher DE (2001) Deformation-enhanced fluctuations in the red cell skeleton with theoretical relations to elasticity, connectivity, and spectrin unfolding. Biophys J 81:3178–3192

Li H, Lykotrafitis G (2012) Two-component coarse-grained molecular-dynamics model for the human erythrocyte membrane. Biophys J 102:75–84

Li H, Lykotrafitis G (2014) Erythrocyte membrane model with explicit description of the lipid bilayer and the spectrin network. Biophys J 107:642–653

Li H, Lykotrafitis G (2015) Vesiculation of healthy and defective red blood cells. Phys Rev E 92(1):012,715

Li H, Zhang Y, Ha V, Lykotrafitis G (2016) Modeling of band-3 protein diffusion in the normal and defective red blood cell membrane. Soft Matter 12(15):3643–3653

Li H, Lu L, Li X, Buffet P, Dao M, Karniadakis GE (2018) Deconvoluting the pathogenic role of spleen in hereditary spherocytosis and elliptocytosis. In preparation

Li J, Dao M, Lim CT, Suresh S (2005) Spectrin-level modeling of the cytoskeleton and optical tweezers stretching of the erythrocyte. Biophys J 88:3707–3719

Li J, Lykotrafitis G, Dao M, Suresh S (2007) Cytoskeletal dynamics of human erythrocyte. Proc Natl Acad Sci USA 104:4937–4942

Li X, Vlahovska PV, Karniadakis GE (2013) Continuum- and particle-based modeling of shapes and dynamics of red blood cells in health and disease. Soft Matter 9:28–37

Li X, Peng Z, Lei H, Dao M, Karniadakis GE (2014) Probing red blood cell mechanics, rheology and dynamics with a two-component multi-scale model. Philos Trans A Math Phys Eng Sci 372:20130,389

Li X, Dao M, Lykotrafitis G, Karniadakis GE (2017a) Biomechanics and biorheology of red blood cells in sickle cell anemia. J Biomech 50:34–41

Li X, Li H, Chang HY, Lykotrafitis G, Karniadakis GE (2017b) Computational biomechanics of human red blood cells in hematological disorders. ASME J Biomech Eng 139:021,008

Malone JG, Johnson NL (1994) A parallel finite-element contact/impact algorithm for nonlinear explicit transient analysis 1. the search algorithm and contact mechanics. Int J Num Meths Engr 37:559–590

McWhirter JL, Noguchi H, Gompper G (2009) Flow-induced clustering and alignment of vesicles and red blood cells in microcapillaries. Proc Natl Acad Sci USA 106(15):6039–6043

Muller K, Fedosov D, Gompper G (2015) Smoothed dissipative particle dynamics with angular momentum conservation. J Comput Phys 281:301–315

Ni A, Cheema TA, Park CW (2015) Numerical study of RBC motion and deformation through microcapillary in alcohol plasma solution. Open J Fluid Dyn 05(01):26–33

Noguchi H, Gompper G (2005) Shape transitions of fluid vesicles and red blood cells in capillary flows. Proc Natl Acad Sci USA 102:14,159–14,164

Pan W, Caswell B, Karniadakis GE (2010) Rheology, microstructure and migration in brownian colloidal suspensions. Langmuir 26(1):133–142

Peng Z, Zhu Q (2013) Deformation of the erythrocyte cytoskeleton in tank treading motions. Soft Matter 9:7617–7627

Peng Z, Asaro R, Zhu Q (2010) Multiscale modeling of erythrocyte membranes. Phys Rev E 81:031,904

Peng Z, Asaro R, Zhu Q (2011) Multiscale modelling of erythrocytes in stokes flow. J Fluid Mech 686:299–337

Peng Z, Li X, Pivkin IV, Dao M, Karniadakis GE, Suresh S (2013) Lipid bilayer and cytoskeletal interactions in a red blood cell. Proc Natl Acad Sci USA 110:13,356–13,361

Peng Z, Mashayekh A, Zhu Q (2014) Erythrocyte responses in low shear rate flows - effects of non-biconcave stress-free state in cytoskeleton. J Fluid Mech 742:96–118

Peng Z, Salehyar S, Zhu Q (2015) Stability of the tank treading modes of erythrocytes and its dependence on cytoskeleton reference states. J Fluid Mech 771:449–467

Peskin CS (2002) The immersed boundary method. Acta Numer 11:479–517

Pivkin IV, Karniadakis GE (2008) Accurate coarse-grained modeling of red blood cells. Phys Rev Lett 101(11):118,105

Pozrikidis C (1992) Boundary integral and singularity methods for linearized viscous flow. Cambridge University Press

Pozrikidis C (2010) Flow-induced deformation of two-dimensional biconcave capsules. In: Computational Hydrodynamics of Capsules and Biological Cells, CRC Press, pp 1–33

Ramanujan S, Pozrikidis C (1998) Deformation of liquid capsules enclosed by elastic membranes in simple shear flow: large deformations and the effect of fluid viscosities. J Fluid Mech 361:117–143

Rief M, Pascual J, Saraste M, Gaub HE (1999) Single molecule force spectroscopy of spectrin repeats: low unfolding forces in helix bundles. J Mol Biol 286:553–561

Shi L, Pan TW, Glowinski R (2014) Three-dimensional numerical simulation of red blood cell motion in poiseuille flows. Int J Numer Methods Fluids 76(7):397–415

Sui Y, Low H, Chew Y, Roy P (2008) Tank-treading, swinging, and tumbling of liquid-filled elastic capsules in shear flow. Phys Rev E 77(1):016,310

Sung LA, Vera C (2003) Protofilament and hexagon: a three-dimensional mechanical model for the junctional complex in the rbc membrane skeleton. Ann Biomed Eng 31:1314–1326

Tang YH, Lu L, Li H, Evangelinos C, Grinberg L, Sachdeva V, Karniadakis GE (2017) Openrbc: A fast simulator of red blood cells atprotein resolution. Biophys J 112(10):2030–2037

Tomishige M (1998) Regulation mechanism of the lateral diffusion of band 3 in erythrocyte membranes by the membrane skeleton. J Cell Biol 142:989–1000

Tran-Son-Tay R, Sutera S, Rao P (1984) Determination of red blood cell membrane viscosity from rheoscopic observations of tank-treading motion. Biophys J 46:65–72

Van Liedekerke P, Odenthal T, Smeets B, Ramon H (2013) Solving microscopic flow problems using stokes equations in sph. Comput Phys Commun 184:1686–1696

Veerapaneni SK, Rahimian A, Biros G, Zorin D (2011) A fast algorithm for simulating vesicle flows in three dimensions. J Comput Phy 230(14):5610–5634

Vlahovska P, Young Y, Danker G, Misbah C (2011) Dynamics of a non-spherical microcapsule with incompressible interface in shear flow. J Fluid Mech 678:221–247

Walensky LD, Mohandas N, Lux SE (2003) Disorders of the red blood cell membrane. In: Handin RI, Lux SE, Stossel TP (eds) Blood: principles and practice of hematology, 2nd ed. Philadelphia, PA: Lippincott Williams & Wilkins, pp 1709–1858

Walter J, Salsac A, Barthès-Biesel D, Tallec PL (2010) Coupling of finite element and boundary integral methods for a capsule in a stokes flow. Int J Numer Meth Engng 83:829–850

Witthoft A, Yazdani A, Peng Z, Bellini C, Humphrey JD, Karniadakis GE (2016) A discrete mesoscopic particle model of the mechanics of a multi-constituent arterial wall. J R Soc Interface 13:20150,964

Yazdani A, Bagchi P (2011) Phase diagram and breathing dynamics of a single red blood cell and a biconcave capsule in dilute shear flow. Phys Rev E 84:026,314

Yazdani A, Kalluri R, Bagchi P (2011) Tank-treading and tumbling frequencies of capsules and red blood cells. Phys Rev E 83:046,305

Zhang Y, Huang C, Kim S, Golkaram M, Dixon MW, Tilley L, Li J, Zhang S, Suresh S (2015) Multiple stiffening effects of nanoscale knobs on human red blood cells infected with plasmodium falciparum malaria parasite. Proc Natl Acad Sci USA 112(19):6068–6073

Zhao H, Isfahania AHG, Olsonc LN, Freund JB (2010) A spectral boundary integral method for flowing blood cells. J Comput Phys 229:3726–3744

Zhu Q, Asaro R (2008) Spectrin folding vs. unfolding reactions and rbc membrane stiffness. Biophys J 94:2529–2545

Zhu Q, Vera C, Asaro R, Sche P, Sung L (2007) A hybrid model for erythrocyte membrane: a single unit of protein network coupled with lipid bilayer. Biophys J 93:386–400